

Axial ligand substitutions in *trans*-bis[1,2-phenylenebis(dimethylarsine)] complexes of ruthenium(II)[†]

Benjamin J. Coe,^{*a} Madeline Chery,^a Roy L. Beddoes,^a Håkon Hope^b and Peter S. White

^a Department of Chemistry, University of Manchester, Oxford Road, Manchester M13 9PL, UK

^b Department of Chemistry, University of California, Davis, California 95616-0935, USA

^c Department of Chemistry, University of North Carolina, Chapel Hill, North Carolina 27599-3290, USA

The series of salts *trans*-[RuCl(pdma)₂L]PF₆ [pdma = 1,2-phenylenebis(dimethylarsine); L = MeCN **1**, pyridine (**2**), 1-methylimidazole (**3**), benzonitrile **4**, 4-ethylpyridine **5**, dimethyl sulfoxide **6**, pyrazine **7** or PPh₃ **8**] were prepared by reaction of *trans*-[RuCl(pdma)₂(NO)]²⁺ with 1 equivalent of NaN₃ in acetone at room temperature followed by reflux with an excess of L in butan-2-one. Reaction of *trans*-[RuCl(pdma)₂(NO)]²⁺ at room temperature in mim afforded the known complex *trans*-[RuCl(NO)₂(pdma)₂]. Methylation of **7** with MeI at room temperature gave *trans*-[RuCl(pdma)₂(mpyz)][PF₆]₂ **9** (mpyz = *N*-methylpyrazinium cation). Treatment of **3** with an excess of NaN₃ in refluxing mim-water afforded *trans*-[Ru(N₃)(pdma)₂(mim)]PF₆ **10** which is converted into *trans*-[Ru(pdma)₂(mim)₂][PF₆]₂ **11** by reaction with NO₂BF₄ in acetone at room temperature, followed by heating in mim. Single-crystal structures of *trans*-[RuCl(NO)₂(pdma)₂], *trans*-[RuCl(pdma)₂(NO)][PF₆]₂, 2-dmf (dmf = dimethylformamide) and **11** have been determined.

The demands inherent in achieving directed syntheses of transition-metal complexes are well established. The ability to exert precise control over ligand substitutions represents an academic challenge, and is a prerequisite for the preparation of complexes designed to exhibit novel properties. Within this field, the development of rational strategies for the synthesis of *trans* octahedral complexes is particularly worthy of attention. Ruthenium is especially attractive in this context because its complexes often exhibit properties such as luminescence¹ or intervalence transfer,² which are of great interest for exploitation in future 'molecular electronic devices'. Although a vast co-ordination chemistry is available,³ few existing ruthenium complexes possess both of the primary requirements for potential synthetic precursors, *i.e.* high stability (with respect to both ligand loss and isomerization) and *trans* ligands which may permit stepwise substitutions. We have chosen to investigate complexes featuring the synthetically accessible, highly stable *trans*-{Ru(pdma)₂}²⁺ [pdma = 1,2-phenylenebis(dimethylarsine)] centre. This system is attractive because it is sterically relatively uncrowded and shows promise for an extensive derivative chemistry.

The complex *trans*-[RuCl(pdma)₂(NO)]²⁺ is readily prepared by reaction of [RuCl₃(NO)]·5H₂O with 2 equivalents of pdma.⁴ The former is a potential synthetic precursor since a *trans* arrangement of nitrosyl and chloride ligands may be amenable to sequential substitutions. The well documented azide-assisted labilization of electrophilic NO ligands is a useful method for generating substituted mono- and polynuclear ruthenium complexes.⁵ Reaction of *trans*-[RuCl(pdma)₂(NO)]²⁺ with an excess of sodium azide is known to afford *trans*-[RuCl(N₃)(pdma)₂],⁶ but the synthesis of further derivatives featuring complete cleavage of the Ru–N bond and/or chloride substitution has not been explored. The object of this study is to develop the axial substitution chemistry of *trans*-[RuCl(pdma)₂(NO)]²⁺ with a view to assessing its potential as a source of functionalized derivatives. The

synthetic knowledge gained is likely to be of relevance to other related ruthenium complexes.

Experimental

Materials and procedures

The compound RuCl₃·2H₂O was supplied by Johnson Matthey plc and pdma was obtained from Dr. P. G. Edwards, University of Wales College of Cardiff. The complex [RuCl₃(NO)]·5H₂O and the salt *trans*-[RuCl(pdma)₂(NO)][PF₆]₂ were prepared according to published procedures.^{†7} The complex *trans*-[RuCl(NO)₂(pdma)₂] was prepared according to a published procedure⁴ and by the method described below. All other reagents were obtained commercially and used as supplied. All reactions were conducted under an argon atmosphere. Products were dried at room temperature in a vacuum desiccator (CaSO₄) for *ca.* 24 h prior to characterization.

Physical measurements

Proton NMR spectra were recorded on a Varian Gemini 200 spectrometer and all shifts are referenced to SiMe₄. Elemental analyses were performed by the Microanalytical Laboratory, University of Manchester. Infrared spectra were obtained as KBr discs with an ATI Mattson Genesis Series FTIR instrument, UV/VIS spectra using a Hewlett Packard 8452A diode-array spectrophotometer and FAB mass spectra using a Kratos Concept spectrometer with a 6–8 keV Xe-atom beam and 3-nitrobenzyl alcohol as matrix.

Cyclic voltammetric measurements were carried out using an EG&G PAR model 173 potentiostat/galvanostat with a model 175 universal programmer. A single-compartment cell was used

[†] See refs. 4 and 6. For *trans*-[RuCl(pdma)₂(NO)]Cl₂: $\nu(\text{NO})$ 1889 vs cm⁻¹, lit.⁸ (for ·1.5H₂O), 1890 vs cm⁻¹ (Found: C, 28.4; H, 4.15; N, 1.55. Calc. for C₂₀H₃₂As₄Cl₃NORu·2H₂O: C, 28.4; H, 4.30; N, 1.65%). For *trans*-[RuCl(pdma)₂(NO)][PF₆]₂: $\nu(\text{NO})$ 1865 vs cm⁻¹, lit.⁸ 1873 vs cm⁻¹ (Found: C, 23.2; H, 3.05; N, 1.35. Calc. for C₂₀H₃₂As₄ClF₁₂NOP₂Ru: C, 23.35; H, 3.15; N, 1.35%).

[†] Non-SI unit employed: eV \approx 1.60 \times 10⁻¹⁹ J.

with a saturated calomel electrode (SCE) as reference separated by a salt bridge from a platinum-bead working electrode and a platinum-wire auxiliary electrode. Acetonitrile (HPLC grade) was used as received and tetra-*n*-butylammonium hexafluorophosphate, twice recrystallized from ethanol and dried *in vacuo*, was used as supporting electrolyte. Solutions containing *ca.* 10^{-3} mol dm⁻³ analyte (0.1 mol dm⁻³ electrolyte) were deaerated for 5 min by a vigorous nitrogen purge. All E_4 values were calculated from $(E_{pa} + E_{pc})/2$ at a scan rate of 200 mV s⁻¹.

Syntheses

***trans*-[RuCl(NO₂)(pdma)₂].** A solution of *trans*-[RuCl(pdma)₂(NO)][PF₆]₂ (100 mg, 0.097 mmol) in 1-methylimidazole (5 cm³) was heated at *ca.* 100 °C for 30 min. After cooling to room temperature, the magenta precipitate was filtered off, washed with water and dried, yield 50 mg (68%). $\nu_{\text{sym}}(\text{NO}_2)$ 1314 vs cm⁻¹ (Found: C, 32.3; H, 3.95; N, 2.05. Calc. for C₂₀H₃₂As₄ClNO₂Ru: C, 31.85; H, 4.25; N, 1.85%). m/z : 755 (M^+), 739 ($[M - O]^{+}$), 725 ($[M - O_2]^{+}$) and 708 ($[M - \text{NO}_2]^{+}$). For *trans*-[RuCl(NO₂)(pdma)₂] prepared by the literature method:⁴ $\nu_{\text{sym}}(\text{NO}_2)$ 1316 vs cm⁻¹ (Found: C, 31.65; H, 4.40; N, 1.85%).

***trans*-[RuCl(pdma)₂(MeCN)]PF₆ 1.** A solution of *trans*-[RuCl(pdma)₂(NO)][PF₆]₂ (200 mg, 0.194 mmol) and NaN₃ (13 mg, 0.200 mmol) in acetonitrile (10 cm³) was stirred at room temperature for 2 h. The pale golden solution was then heated at reflux for 3 h, cooled to room temperature and the solvent removed *in vacuo*. The resulting pale yellow oil was dissolved in acetone (2 cm³), and addition of aqueous NH₄PF₆ afforded a pale precipitate which was filtered off, washed with water and dried. Purification was effected by filtration through Celite in acetone followed by slow precipitation with diethyl ether to yield a cream microcrystalline solid, yield 172 mg (90%). $\delta_{\text{H}}(\text{CD}_3\text{COCD}_3)$ 8.22 (4 H, m, 2C₆H₂), 7.76 (4 H, m, 2C₆H₂), 2.30 (3 H, s, MeCN), 1.88 (12 H, s, 4AsMe) and 1.87 (12 H, s, 4AsMe). $\nu(\text{C}\equiv\text{N})$ 2267 vw cm⁻¹ (Found: C, 32.15; H, 4.25; N, 1.45. Calc. for C₂₂H₃₅As₄ClF₆NPRu·1.5C₃H₆O: C, 32.4; H, 4.50; N, 1.45%). m/z : 750 ($[M - \text{PF}_6^-]^{+}$).

***trans*-[RuCl(pdma)₂(py)]PF₆ 2.** A solution of *trans*-[RuCl(pdma)₂(NO)][PF₆]₂ (100 mg, 0.097 mmol) and NaN₃ (6.5 mg, 0.100 mmol) in pyridine (py) (5 cm³) was stirred at room temperature for 2 h. The golden solution was heated at *ca.* 100 °C for 1 h, then cooled to room temperature, and addition of aqueous NH₄PF₆ afforded a pale golden precipitate. This was filtered off, washed with water and dried. The product was purified in the same manner as for **1** to yield a pale golden microcrystalline solid, yield 88 mg (92%). $\delta_{\text{H}}(\text{CD}_3\text{COCD}_3)$ 8.31 (4 H, m, 2C₆H₂), 7.83 (4 H, m, 2C₆H₂), 7.69–7.64 (3 H, m, H^{2,4,6}), 7.07 (2 H, t, H^{3,5}), 1.90 (12 H, s, 4AsMe) and 1.75 (12 H, s, 4AsMe) (Found: C, 33.7; H, 3.70; N, 1.40. Calc. for C₂₅H₃₇As₄ClF₆NPRu·C₃H₆O: C, 33.95; H, 4.35; N, 1.4%). m/z : 788 ($[M - \text{PF}_6^-]^{+}$).

***trans*-[RuCl(pdma)₂(mim)]PF₆ 3.** A solution of *trans*-[RuCl(pdma)₂(NO)][PF₆]₂ (200 mg, 0.194 mmol) and NaN₃ (13 mg, 0.200 mmol) in acetone (5 cm³) was stirred at room temperature for 2 h. 1-Methylimidazole (mim) (5 cm³) was added, and the acetone was removed *in vacuo*. The golden solution was heated at *ca.* 100 °C for 1 h, then cooled to room temperature, and addition of aqueous NH₄PF₆ afforded a pale golden precipitate. This was filtered off, washed with water and dried. The product was purified in the same manner as for **1** to yield a pale amber solid, yield 158 mg (87%). $\delta_{\text{H}}(\text{CD}_3\text{COCD}_3)$ 8.27 (4 H, m, 2C₆H₂), 7.79 (4 H, m, 2C₆H₂), 6.93 (1 H, s, C₃H₃N₂Me), 6.89 (1 H, t, *J* 1.4, C₃H₃N₂Me), 5.74 (1 H, t, *J* 1.4 Hz, C₃H₃N₂Me), 3.54 (3 H, s, Me of mim), 1.83 (12 H, s, 4AsMe) and 1.73 (12 H, s, 4AsMe) (Found: C, 31.05; H, 4.05; N, 3.05.

Calc. for C₂₄H₃₈As₄ClF₆N₂PRu: C, 30.8; H, 4.10; N, 3.00%). m/z : 791 ($[M - \text{PF}_6^-]^{+}$).

***trans*-[RuCl(pdma)₂(PhCN)]PF₆ 4.** This was synthesized in a similar manner to that of salt **3** by using *trans*-[RuCl(pdma)₂(NO)][PF₆]₂ (100 mg, 0.097 mmol), NaN₃ (6.5 mg, 0.100 mmol) and benzonitrile in place of 1-methylimidazole. The crude product was precipitated by addition of diethyl ether, filtered off, washed with diethyl ether and dried. Purification was effected by filtration through Celite in acetone followed by precipitation with aqueous NH₄PF₆. The pale yellow product was filtered off, washed with water and dried, yield 92 mg (99%). $\delta_{\text{H}}(\text{CD}_3\text{COCD}_3)$ 8.25 (4 H, m, 2C₆H₂), 7.77 (4 H, m, 2C₆H₂), 7.66–7.55 (1 H, m, H⁴), 7.54–7.40 (4 H, m, H^{2,3,5,6}) and 1.96 (24 H, s, 8AsMe). $\nu(\text{C}\equiv\text{N})$ 2221 m cm⁻¹ (Found: C, 33.95; H, 4.00; N, 1.40. Calc. for C₂₇H₃₇As₄ClF₆NPRu: C, 33.9; H, 3.90; N, 1.45%). m/z : 812 ($[M - \text{PF}_6^-]^{+}$).

***trans*-[RuCl(pdma)₂(epy)]PF₆ 5.** This was synthesized and purified in identical manner to that of salt **4** by using 4-ethylpyridine (epy) in place of benzonitrile. The product was finally precipitated from acetone–diethyl ether to give a pale golden microcrystalline solid, yield 72 mg (77%). $\delta_{\text{H}}(\text{CD}_3\text{COCD}_3)$ 8.30 (4 H, m, 2C₆H₂), 7.82 (4 H, m, 2C₆H₂), 7.46 (2 H, d, *J* 6.6, C₅H₄NEt), 6.94 (2 H, d, *J* 6.9, C₅H₄NEt), 2.51 (2 H, q, *J* 7.6, CH₂CH₃ of epy), 1.89 (12 H, s, 4AsMe), 1.74 (12 H, s, 4AsMe) and 1.04 (3 H, t, *J* 7.6 Hz, CH₂CH₃ of epy) (Found: C, 34.05; H, 4.10; N, 1.50. Calc. for C₂₇H₄₁As₄ClF₆NPRu: C, 33.75; H, 4.30; N, 1.45%). m/z : 816 ($[M - \text{PF}_6^-]^{+}$).

***trans*-[RuCl(pdma)₂(dmsO)]PF₆ 6.** This was synthesized and purified in a manner identical to that of salt **3** by using dimethyl sulfoxide (dmsO) in place of 1-methylimidazole, affording a white solid, yield 85 mg (94%). $\delta_{\text{H}}(\text{CD}_3\text{COCD}_3)$ 8.15 (4 H, m, 2C₆H₂), 7.74 (4 H, m, 2C₆H₂), 2.97 (6 H, s, dmsO), 2.20 (12 H, s, 4AsMe) and 1.84 (12 H, s, 4AsMe). $\nu(\text{S}=\text{O})$ 1083 m and 1011 m cm⁻¹ (Found: C, 28.35; H, 4.15; S, 3.35. Calc. for C₂₂H₃₈As₄ClF₆OPRuS: C, 28.35; H, 4.10; S, 3.45%). m/z : 787 ($[M - \text{PF}_6^-]^{+}$).

***trans*-[RuCl(pdma)₂(pyz)]PF₆ 7.** A solution of *trans*-[RuCl(pdma)₂(NO)][PF₆]₂ (100 mg, 0.097 mmol) and NaN₃ (6.5 mg, 0.100 mmol) in acetone (5 cm³) was stirred at room temperature for 2 h. Butan-2-one (10 cm³) and pyrazine (pyz) (322 mg, 4.02 mmol) were added and the acetone was removed *in vacuo*. The solution was heated at reflux for 2 h to give a bright golden solution. The solvent was removed *in vacuo* until *ca.* 1 cm³ remained, and diethyl ether was added to give a golden precipitate which was filtered off, washed with diethyl ether and dried. The solid was dissolved in acetone, filtered through Celite, and precipitated by addition of water. The bright golden product was filtered off, washed with water and dried, yield 84 mg (93%). $\delta_{\text{H}}(\text{CD}_3\text{COCD}_3)$ 8.31 (4 H, m, 2C₆H₂), 8.13 (2 H, d, *J* 4.2 Hz, pyz), 7.88–7.80 (6 H, m, 2C₆H₂ and pyz), 1.91 (12 H, s, 4AsMe) and 1.81 (12 H, s, 4AsMe) (Found: C, 30.8; H, 4.20; N, 3.15. Calc. for C₂₄H₃₆As₄ClF₆N₂PRu: C, 30.85; H, 3.90; N, 3.00%). m/z : 789 ($[M - \text{PF}_6^-]^{+}$).

***trans*-[RuCl(pdma)₂(PPh₃)]PF₆ 8.** This was prepared and purified in similar manner to that of salt **7** by using triphenylphosphine (624 mg, 2.38 mmol) in place of pyrazine. The product was obtained as a cream powder, yield 95.5 mg (88%). $\delta_{\text{H}}(\text{CD}_3\text{COCD}_3)$ 8.11 (4 H, m, 2C₆H₂), 7.82 (4 H, m, 2C₆H₂), 7.48–7.37 (3 H, m, 3 H⁴), 7.23–7.14 (6 H, m, 3 H^{3,5}), 6.94–6.84 (6 H, m, 3 H^{2,6}), 1.75 (12 H, s, 4AsMe) and 1.43 (12 H, s, 4AsMe) (Found: C, 41.6; H, 4.85; P, 5.0. Calc. for C₃₈H₄₇As₄ClF₆P₂Ru·C₃H₆O: C, 41.95; H, 4.55; P, 5.30%). m/z : 970 ($[M - \text{PF}_6^-]^{+}$).

trans-[RuCl(pdma)₂(mpyz)][PF₆]₂ 9 (mpyz = *N*-methylpyrazinium). To a solution of salt 7 (50 mg, 0.054 mmol) in dimethylformamide (dmf) (1.5 cm³) was added methyl iodide (1.5 cm³). The mixture was stirred at room temperature for 26 h. The excess of methyl iodide was removed *in vacuo* and addition of aqueous NH₄PF₆ afforded a dark precipitate. This was filtered off, washed with water and dried. The crude product was dissolved through the frit in acetone, leaving a tan residue. Addition of diethyl ether to the purple filtrate solution caused precipitation of the product which was filtered off and washed with diethyl ether. The product was precipitated once more from acetone–diethyl ether to afford a deep purple microcrystalline solid, yield 26 mg (43%). δ_H(CD₃COCD₃) 8.74 (2 H, d, *J* 5.2, pyz), 8.31 (4 H, m, 2C₆H₂), 8.25 (2 H, d, *J* 5.1 Hz, pyz), 7.86 (4 H, m, 2C₆H₂), 4.01 (3 H, s, Me of mpyz), 1.95 (12 H, s, 4AsMe) and 1.92 (12 H, s, 4AsMe) (Found: C, 28.5; H, 3.90; N, 2.55. Calc. for C₂₅H₃₉As₄ClF₁₂N₂P₂Ru·0.5C₃H₆O: C, 28.35; H, 3.75; N, 2.50%). *m/z*: 948 ([*M* – PF₆[–]]⁺) and 804 ([*M* – 2PF₆[–]]⁺).

trans-[Ru(N₃(pdma)₂(mim))PF₆ 10. A solution of salt 3 (100 mg, 0.107 mmol) and NaN₃ (3.21 g, 49.4 mmol) in 1-methylimidazole (4 cm³) and water (10 cm³) was stirred at reflux for 24 h. The mixture was cooled in a refrigerator and a small amount of pale solid was filtered off and washed with water. The crude product was obtained by addition of aqueous NH₄PF₆ to the pale yellow filtrate. The precipitate was filtered off, washed with water and dried. Purification was effected by passage through a short column of silica gel in 20% acetone–dichloromethane. The product was then precipitated by addition of diethyl ether, filtered off, washed with diethyl ether and dried to afford a very pale yellow solid, yield 85 mg (84%). δ_H(CD₃COCD₃) 8.29 (4 H, m, 2C₆H₂), 7.81 (4 H, m, 2C₆H₂), 6.88 (1 H, t, *J* 1.5, C₃H₃N₂Me), 6.83 (1 H, s, C₃H₃N₂Me), 5.68 (1 H, t, *J* 1.5 Hz, C₃H₃N₂Me), 3.51 (3 H, s, Me of mim), 1.89 (12 H, s, 4AsMe) and 1.76 (12 H, s, 4AsMe). ν(N₃) 2043s cm^{–1} (Found: C, 30.5; H, 4.45; N, 7.30. Calc. for C₂₄H₃₈As₄F₆N₅PRu: C, 30.6; H, 4.05; N, 7.45%). *m/z*: 798 ([*M* – PF₆[–]]⁺) and 688 ([*M* – PF₆[–] – mim – N₃]⁺).

trans-[Ru(pdma)₂(mim)₂][PF₆]₂ 11. To a solution of salt 10 (100 mg, 0.106 mmol) in acetone (5 cm³) was added NO₂BF₄ (20 mg, 0.151 mmol). The solution immediately turned green, but after 15 min stirring in air it returned to pale yellow. Addition of aqueous NH₄PF₆ afforded a pale precipitate which was filtered off, washed with water and dried (102 mg). This material was dissolved in 1-methylimidazole (5 cm³) and heated at *ca.* 100 °C for 1 h. Addition of aqueous NH₄PF₆ afforded a pale yellow precipitate which was filtered off, washed with water and dried. Purification was effected by washing with dichloromethane followed by passage through a short silica gel column in acetone. The product was finally recrystallized several times from acetonitrile–diethyl ether to afford almost colourless crystals, yield 60 mg (50%). δ_H(CD₃COCD₃) 8.41 (4 H, m, 2C₆H₂), 7.91 (4 H, m, 2C₆H₂), 7.03 (2 H, d, *J* 1.4, 2C₃H₃N₂Me), 7.00 (2 H, t, *J* 1.5, 2C₃H₃N₂Me), 5.82 (2 H, t, *J* 1.5 Hz, 2C₃H₃N₂Me), 3.57 (6 H, s, 2 Me of mim) and 1.79 (24 H, s, 8AsMe) (Found: C, 30.0; H, 3.80; N, 5.25. Calc. for C₂₈H₄₄As₄F₁₂N₄P₂Ru: C, 29.85; H, 3.95; N, 4.95%). *m/z*: 982 ([*M* – PF₆[–]]⁺), 837 ([*M* – 2PF₆[–]]⁺), 755 ([*M* – 2PF₆[–] – mim]⁺) and 674 ([*M* – 2PF₆[–] – 2mim]⁺).

Crystallography

Crystals of *trans*-[RuCl(NO₂)(pdma)₂] were grown by warming a solution of *trans*-[RuCl(pdma)₂(NO)][PF₆]₂ in 1-methylimidazole to 75 °C and maintaining the temperature for 3 h. They are flat, thin needles. The central lengthwise portion appears irregular in polarized light. The crystal used for diffraction study, having dimensions 0.18 × 0.06 × 0.02 mm,

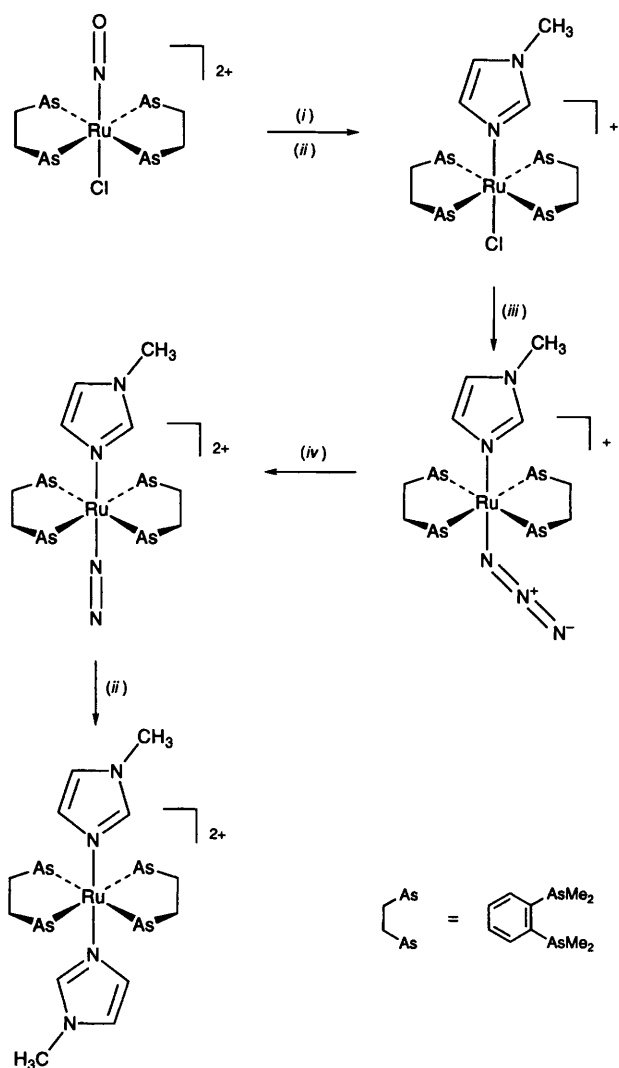
was obtained by cutting out one side of a needle to provide a sample of homogeneous appearance. This was attached to a thin glass fibre with vacuum grease and placed in the cold stream of a locally modified Siemens LT-2 device. All crystals examined were twinned *via* a 180° rotation around the *a* axis; reflections corresponding to one twin partner were resolved and measured using a Siemens P4/RA diffractometer. The structure was solved using the Patterson instruction of SHELXS 86,⁹ and refined using full-matrix least squares on *F*_o² for all unique reflections (SHELXL 93).¹⁰ Data were corrected for absorption using the program XABS 2¹¹ with maximum and minimum transmission factors of 0.90 and 0.58. The non-hydrogen atoms were refined anisotropically and hydrogen atoms were included in idealized positions. The Cl and NO₂ ligands are disordered across an inversion centre, resulting in nearly equal positional parameters for both. The atoms of these ligands were fixed at 50% occupancy with the other 50% being generated by the inversion centre. The O atoms were resolved. The geometry of the NO₂ group was held fixed during refinement, allowing the assignment of individual positional parameters for Cl and N.

Crystals of *trans*-[RuCl(pdma)₂(py)]PF₆·dmf (2·dmf) were grown by diffusion of diethyl ether vapour into a dmf solution at room temperature. A yellow prismatic crystal of dimensions 0.07 × 0.10 × 0.20 mm was mounted on a glass fibre and data were collected on a Rigaku AFC5R diffractometer at ambient temperature. The structure was solved by direct methods with SHELXS 86,⁹ and refined using full-matrix least squares on *F*_o for all unique reflections with correction for Lorentz-polarization factors (TEXSAN).¹² Data were corrected for absorption using the program DIFABS¹³ with maximum and minimum transmission factors of 1.38 and 0.82. The non-hydrogen atoms were refined anisotropically and hydrogen atoms were included in idealized positions. A molecule of dmf of crystallization was refined as far as possible to a satisfactory shape and then fixed to permit smooth convergence of the least-squares refinement. The location close to a two-fold axis and large *B*_{eq} values suggest partial occupancy.

Crystals of *trans*-[RuCl(pdma)₂(NO)][PF₆]₂ and *trans*-[Ru(pdma)₂(mim)₂][PF₆]₂ 11 were grown by diffusion of diethyl ether vapour into acetonitrile solutions at room temperature. A pale yellow crystal of *trans*-[RuCl(pdma)₂(NO)][PF₆]₂ having dimensions 0.40 × 0.35 × 0.25 mm and a colourless crystal of 11 of dimensions 0.35 × 0.30 × 0.40 mm were selected for diffraction study and data were collected on a Rigaku AFC6S diffractometer at low temperature. The structures were solved using the NRCVAX suite of programs,¹⁴ and refined using full-matrix least squares on *F*_o for all unique reflections. Data were corrected for absorption using ABSORP,¹⁴ maximum and minimum transmission factors being 0.36 and 0.14 for *trans*-[RuCl(pdma)₂(NO)][PF₆]₂ and 0.43 and 0.28 for 11. The non-hydrogen atoms were refined anisotropically and hydrogen atoms were included in idealized positions. The cation *trans*-[RuCl(pdma)₂(NO)]²⁺ is disordered analogously to *trans*-[RuCl(NO₂)(pdma)₂], with Cl(1) and N(1)–O(1) being superimposed. Each of these atoms was fixed at 50% occupancy with the other 50% being generated by the inversion centre. The Ru(1)–N(1) distance was fixed at 1.750 Å, corresponding to the mean value taken from 18 linear *trans*-Cl–Ru–N=O fragments found in the Cambridge Structural Database (Ru–N 1.703–1.810 Å), and Cl(1) and O(1) were allowed to move. For 11 the unit cell contains two crystallographically non-equivalent molecules each occupying a centre of symmetry.

The ORTEP¹⁵ diagrams showing views of the complexes are given in Figs. 1–4. Crystallographic data and refinement details are presented in Table 6, and selected bond distances and angles in Tables 2–5.

Atomic coordinates, thermal parameters, and bond lengths and angles have been deposited at the Cambridge Crystallo-



Scheme 1 Synthesis of the complex in **11** in four steps starting from $\text{trans-}[\text{RuCl}(\text{pdma})_2(\text{NO})][\text{PF}_6]_2$: (i) NaN_3 (1 equivalent); (ii) excess of mim; (iii) excess of NaN_3 ; (iv) NO_2BF_4

graphic Data Centre (CCDC). See Instructions for Authors, *J. Chem. Soc., Dalton Trans.*, 1996, Issue 1. Any request to the CCDC for this material should quote the full literature citation and the reference number 186/210.

Results and Discussion

Synthetic studies

The reaction of $\text{trans-}[\text{RuCl}(\text{pdma})_2(\text{NO})]^{2+}$ with hydroxide ion either in water or in methanol containing an amine to form the highly insoluble, pale yellow complex $\text{trans-}[\text{RuCl}(\text{NO}_2)(\text{pdma})_2]$ has been reported previously.⁴ This reaction also occurs in 1-methylimidazole, although the identity of the product was initially uncertain owing to its strong pink colour. The production of $\text{trans-}[\text{RuCl}(\text{NO}_2)(\text{pdma})_2]$, indicated by infrared spectra and elemental analyses, is confirmed by X-ray diffraction (see below). The pink colour is apparently due to an unidentified trace impurity, possibly a dimeric complex, which co-crystallizes with $\text{trans-}[\text{RuCl}(\text{NO}_2)(\text{pdma})_2]$. Treatment of pink $\text{trans-}[\text{RuCl}(\text{NO}_2)(\text{pdma})_2]$ with aqueous HCl returns pure $\text{trans-}[\text{RuCl}(\text{pdma})_2(\text{NO})]^{2+}$ in high yield.

The nitrosyl ligand in $\text{trans-}[\text{RuCl}(\text{pdma})_2(\text{NO})]^{2+}$ reacts completely with 1 equivalent of azide ion at room temperature to afford primarily the previously reported dinitrogen complex $\text{trans-}[\text{RuCl}(\text{pdma})_2(\text{N}_2)]^{2+}$.^{4,6} Isolation of the latter in pure form by using this method was unsuccessful,* but *in situ* treatment with a pro-ligand either as solvent or in refluxing

butan-2-one leads to clean, high-yield formation of monosubstituted derivatives, $\text{trans-}[\text{RuCl}(\text{pdma})_2\text{L}]\text{PF}_6$ (L = MeCN **1**, py **2**, mim **3**, PhCN **4**, epy **5**, dmsO **6**, pyz **7** or PPh_3 **8**). The reflux temperature of acetone is insufficient to give efficient cleavage of the Ru–N bond, in accord with the reported stability of $\text{trans-}[\text{RuCl}(\text{pdma})_2(\text{N}_2)]^{2+}$.^{4,6} This behaviour provides a marked contrast with the reactivity of the related complex $\text{trans-}[\text{RuCl}(\text{py})_4(\text{NO})]^{2+}$. Treatment of the latter with stoichiometric azide ion in acetone leads to rupture of the Ru–N bond, forming a labile solvent complex which reacts at room temperature to give derivatives $\text{trans-}[\text{RuCl}(\text{py})_4\text{L}]^{2+}$ (L = py, etc.).^{5c} Clearly, the axial ruthenium–ligand bond strengths are markedly influenced by the equatorial ligands.

The chloride in derivatives $\text{trans-}[\text{RuCl}(\text{pdma})_2\text{L}]^{2+}$ (L = MeCN or mim) is remarkably inert to substitution by neutral ligands, even in the presence of silver(I) ion.† However, reaction does occur with azide ion, and complete chloride replacement is achieved under sufficiently forcing conditions, producing the azido complex $\text{trans-}[\text{Ru}(\text{N}_3)(\text{pdma})_2(\text{mim})]^{2+}$ (**10**) in high yield. During some attempts at purification **10** was found to undergo slow conversion into another complex in solution, as observed by ¹H NMR spectroscopy. This product is likely to be the nitro complex $\text{trans-}[\text{Ru}(\text{NO}_2)(\text{pdma})_2(\text{mim})]^{2+}$, since the related azido complex $\text{trans-}[\text{RuCl}(\text{N}_3)(\text{pdma})_2]$ reportedly reacts with air in the presence of light to give $\text{trans-}[\text{RuCl}(\text{NO}_2)(\text{pdma})_2]$.⁴

The complex $\text{trans-}[\text{Ru}(\text{N}_3)(\text{pdma})_2(\text{mim})]^{2+}$ undergoes rapid reaction with a slight excess of nitronium tetrafluoroborate to afford primarily the dinitrogen complex $\text{trans-}[\text{Ru}(\text{N}_2)(\text{pdma})_2(\text{mim})]^{2+}$. This reaction parallels that of $\text{trans-}[\text{RuCl}(\text{N}_3)(\text{pdma})_2]$ with NO_2SbF_6 to give $\text{trans-}[\text{RuCl}(\text{N}_2)(\text{pdma})_2]^{2+}$.⁶ Proton NMR spectroscopy shows that at least one other complex is produced, and it is not possible to achieve a clean conversion into $\text{trans-}[\text{Ru}(\text{N}_2)(\text{pdma})_2(\text{mim})]^{2+}$ via this method.‡ The use of a larger excess of NO_2BF_4 leads to the formation of other impurities, possibly due to nitration of the pdma or mim ligands.

The dinitrogen ligand in $\text{trans-}[\text{Ru}(\text{N}_2)(\text{pdma})_2(\text{mim})]^{2+}$ is readily substituted by 1-methylimidazole to give a disubstituted derivative isolated as the salt $\text{trans-}[\text{Ru}(\text{pdma})_2(\text{mim})_2][\text{PF}_6]_2$ **11** in reasonable yield. This reaction completes the pathway for sequential substitution at the $\text{trans-}\{\text{Ru}(\text{pdma})_2\}^{2+}$ centre in a total of four steps starting from $\text{trans-}[\text{RuCl}(\text{pdma})_2(\text{NO})]^{2+}$ (Scheme 1).

¹H NMR studies

The presence of the *trans* geometry at the $\{\text{Ru}(\text{pdma})_2\}^{2+}$ centre is readily established by simple but informative ¹H NMR

* Addition of aqueous NH_4PF_6 to the reaction solution afforded a pale yellow precipitate which turned pale brown on filtration and drying. Exposure to air caused a further change to pale pink. This material was found to contain $\text{trans-}[\text{RuCl}(\text{pdma})_2(\text{N}_2)]\text{PF}_6$, as shown by infrared spectroscopy: $\nu(\text{N}_2)$ 2132m, lit.,^{4,6} 2130s cm^{-1} . Proton NMR spectroscopy showed significant contamination by at least two other $\text{trans-}\{\text{Ru}(\text{pdma})_2\}^{2+}$ complexes, and the N analysis of 1.4% is lower than that expected (3.20%) for pure $\text{trans-}[\text{RuCl}(\text{pdma})_2(\text{N}_2)]\text{PF}_6$.

† Treatment of complex **3** with AgO_2CCF_3 in mim at ca. 100 °C for 1 h did lead to some precipitation of AgCl. However, 80% of the starting material was recovered unreacted, and that which had reacted formed an insoluble material, indicating decomposition rather than the desired chloride substitution.

‡ The dinitrogen complex was isolated in impure form only and resisted attempts at purification. Spectral data for $\text{trans-}[\text{Ru}(\text{N}_2)(\text{pdma})_2(\text{mim})][\text{PF}_6]_2$: $\delta_{\text{H}}(\text{CD}_3\text{COCD}_3)$ 8.42 (4 H, m, C_6H_2), 7.93 (4 H, m, C_6H_2), 7.11 (1 H, t, J 1.5, $\text{C}_3\text{H}_3\text{N}_2\text{Me}$), 7.05 (1 H, s, $\text{C}_3\text{H}_3\text{N}_2\text{Me}$), 5.89 (1 H, t, J 1.6 Hz, $\text{C}_3\text{H}_3\text{N}_2\text{Me}$), 3.55 (3 H, s, Me of mim), 2.16 (12 H, s, 4AsMe) and 1.99 (12 H, s, 4AsMe); $\nu(\text{N}_2)$ 2170m cm^{-1} . Likely by-products of the reaction between $\text{trans-}[\text{Ru}(\text{N}_3)(\text{pdma})_2(\text{mim})]^{2+}$ and NO_2BF_4 are $\text{trans-}[\text{Ru}(\text{N}_2\text{O})(\text{pdma})_2(\text{mim})]^{2+}$ and $\text{trans-}[\text{Ru}(\text{pdma})_2(\text{mim})(\text{NO})]^{3+}$.

Table 1 The UV/VIS and electrochemical data in acetonitrile

Complex salt	E_3/V vs. SCE ($\Delta E_p/mV$) ^a		λ_{max}/nm ($\epsilon/dm^3 mol^{-1} cm^{-1}$)	Assignment
	Ru ^{II} -Ru ^{III}	Other waves		
<i>trans</i> -[RuCl(pdma) ₂ (NO)][PF ₆] ₂		0.06 (65) -0.47 (115) -1.59 (100)	220 (42 500) 260 (36 900) 328 (sh) (1500)	$\pi \rightarrow \pi^*$ $\pi \rightarrow \pi^*$ $d \rightarrow d, d_{\pi} \rightarrow \pi^*(NO)$
1 <i>trans</i> -[RuCl(pdma) ₂ (MeCN)]PF ₆	1.14 (65)		220 (39 100) 270 (sh) (2400) 354 (240)	$\pi \rightarrow \pi^*$ $\pi \rightarrow \pi^*$ $d \rightarrow d$
2 <i>trans</i> -[RuCl(pdma) ₂ (py)]PF ₆	1.07 (70)		220 (25 000) 292 (2200) 360 (5300)	$\pi \rightarrow \pi^*$ $\pi \rightarrow \pi^*$ $d_{\pi} \rightarrow \pi^*(py)$
3 <i>trans</i> -[RuCl(pdma) ₂ (mim)]PF ₆	0.87 (65)		222 (30 000) 268 (sh) (2600) 368 (sh) (90)	$\pi \rightarrow \pi^*$ $\pi \rightarrow \pi^*$ $d \rightarrow d$
4 <i>trans</i> -[RuCl(pdma) ₂ (PhCN)]PF ₆	1.21 (70)		224 (23 900) 236 (24 900) 322 (10 800)	$\pi \rightarrow \pi^*$ $\pi \rightarrow \pi^*$ $d_{\pi} \rightarrow \pi^*(PhCN)$
5 <i>trans</i> -[RuCl(pdma) ₂ (epy)]PF ₆	1.04 (75)		220 (22 200) 292 (2700) 352 (6800)	$\pi \rightarrow \pi^*$ $\pi \rightarrow \pi^*$ $d_{\pi} \rightarrow \pi^*(epy)$
6 <i>trans</i> -[RuCl(pdma) ₂ (dmsO)]PF ₆	1.73 ^b 0.76 ^c	-1.83 ^c	236 (21 400) 288 (sh) (650) 326 (sh) (410)	$\pi \rightarrow \pi^*$ $d \rightarrow d$ $d \rightarrow d$
7 <i>trans</i> -[RuCl(pdma) ₂ (pyz)]PF ₆	1.20 (70)	-1.50 ^c	220 (28 700) 256 (7000) 280 (sh) (2500)	$\pi \rightarrow \pi^*$ $\pi \rightarrow \pi^*$ $\pi \rightarrow \pi^*$
8 <i>trans</i> -[RuCl(pdma) ₂ (PPh ₃)]PF ₆	1.44 (230)		422 (6100) 220 (32 100) 240 (40 200) 308 (1300)	$d_{\pi} \rightarrow \pi^*(pyz)$ $\pi \rightarrow \pi^*$ $\pi \rightarrow \pi^*$ $d \rightarrow d$
9 <i>trans</i> -[RuCl(pdma) ₂ (mpyz)][PF ₆] ₂	1.46 (75)	-0.37 (65) -1.45 ^c	364 (600) 218 (20 000) 234 (21 700) 278 (6100) 350 (1300)	$d \rightarrow d$ $\pi \rightarrow \pi^*$ $\pi \rightarrow \pi^*$ $\pi \rightarrow \pi^*$ $d \rightarrow d$
10 <i>trans</i> -[Ru(N ₃)(pdma) ₂ (mim)]PF ₆	0.71 (60)		558 (12 000) 220 (16 500) 286 (sh) (3300)	$d_{\pi} \rightarrow \pi^*(mpyz)$ $\pi \rightarrow \pi^*$ $\pi \rightarrow \pi^*$
11 <i>trans</i> -[Ru(pdma) ₂ (mim) ₂][PF ₆] ₂	1.25 (70)		360 (sh) (490) 220 (24 300) 264 (6600) 338 (sh) (220)	$d \rightarrow d$ $\pi \rightarrow \pi^*$ $\pi \rightarrow \pi^*$ $d \rightarrow d$

^a Measured in solutions *ca.* $10^{-3} mol dm^{-3}$ in complex salt and $0.1 mol dm^{-3}$ in NBu_4PF_6 at a platinum-bead working electrode with a scan rate of $200 mV s^{-1}$. Ferrocene internal reference $E_3 = 0.41 V$, $\Delta E_p = 60 mV$. ^b E_{pa} for an irreversible oxidation process. ^c E_{pc} for an irreversible reduction process.

spectra. These exhibit a characteristic AA'BB' pattern of multiplets for the eight benzene ring protons together with two singlets for the 24 protons of the $AsMe_2$ groups. The positions of all of these signals are sensitive to the nature of the axial ligands, with the methyl resonances occurring over a range of *ca.* 1.1 ppm, and showing a separation of between 0 (in **4**) and 0.36 (in **6**) ppm.

FAB mass spectrometric studies

All Ru-containing fragments give broad isotope envelopes; the m/z values quoted are for the most intense peaks which may not correspond precisely with those calculated from relative atomic masses. All complexes give intense molecular ion signals, and also observed for *trans*-[RuCl(NO₂)(pdma)₂] and for **1-9** is an envelope centred at $m/z = 709$ corresponding to the [RuCl(pdma)₂]⁺ fragment.

UV/VIS studies

Spectra for all of the new complex salts were recorded in acetonitrile and data are presented in Table 1. Complexes containing π -acceptor ligands show intense, broad $d_{\pi}(Ru^{II}) \rightarrow \pi^*(L)$ metal-to-ligand charge-transfer (m.l.c.t.) bands in the region 320–560 nm. The m.l.c.t. energy increases predictably

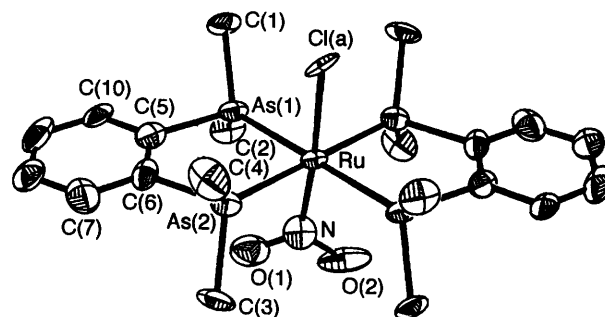


Fig. 1 Structural representation of *trans*-[RuCl(NO₂)(pdma)₂] with disorder removed and hydrogen atoms omitted. The thermal ellipsoids correspond to 50% probability

in the order $mpyz < pyz < py < epy < NO < PhCN$, corresponding to a raising in energy of the π^* ligand lowest unoccupied molecular orbital (LUMO). Methylation of the free pyrazine nitrogen in **7** to give **9** produces a red shift of 136 nm in the m.l.c.t. band, accompanied by a doubling in intensity. This compares with a red shift of 66 nm and a negligible intensity difference between the complexes [Ru(NH₃)₅(pyz)]²⁺ and [Ru(NH₃)₅(mpyz)]³⁺ in aqueous solution.¹⁶

In cases where they are not obscured by the m.l.c.t. bands, weak-to-medium-intensity bands are observed in the region

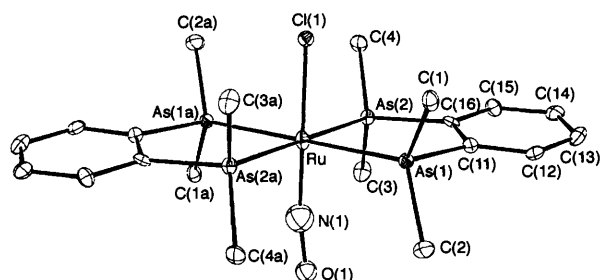


Fig. 2 Structural representation of the cation $trans\text{-}[\text{RuCl}(\text{pdma})_2(\text{NO})]^{2+}$, details as in Fig. 1

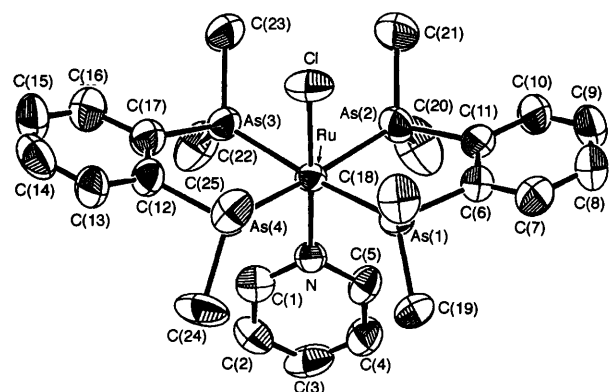


Fig. 3 Structural representation of the cation in salt 2-dmf, $trans\text{-}[\text{RuCl}(\text{pdma})_2(\text{py})]^+$, with hydrogen atoms omitted. The thermal ellipsoids correspond to 50% probability

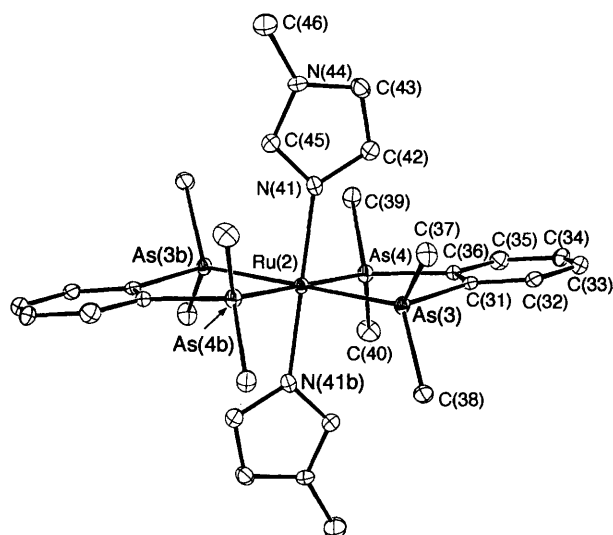


Fig. 4 Structural representation of one of the two crystallographically non-equivalent cations in salt 11, $trans\text{-}[\text{Ru}(\text{pdma})_2(\text{mim})_2]^{2+}$, with hydrogen atoms omitted. The thermal ellipsoids correspond to 50% probability

280–370 nm. These are assigned to spin-allowed $d \rightarrow d$ transitions, by comparison with data for other ruthenium(II) complexes.¹⁷ In addition to the $d \rightarrow d$ and m.l.c.t. bands, all of the complexes also show intense, high-energy bands due to intraligand $\pi \rightarrow \pi^*$ excitations.

Electrochemical studies

The electrochemical properties of the complexes were studied by cyclic voltammetry in acetonitrile, and results are given in Table 1. The precursor $trans\text{-}[\text{RuCl}(\text{pdma})_2(\text{NO})][\text{PF}_6]_2$ shows a reversible wave at 0.06 V *vs.* SCE, assigned to a one-electron reduction of the $\{\text{Ru}(\text{NO})\}^6$ moiety.¹⁸ Two further,

Table 2 Selected bond distances (Å) and angles (°) for $trans\text{-}[\text{RuCl}(\text{NO})_2(\text{pdma})_2]$

Ru–N	2.045(14)	Ru–Cl	2.448(9)
Ru–As(1)	2.416(2)	N–O(1)	1.225(3)
Ru–As(2)	2.406(2)	N–O(2)	1.225(3)
As(1)–Ru–As(2)	84.31(6)	N–Ru–Cl(a)	175.0(8)
As(1)–Ru–Cl(a)	91.0(2)	O(1)–N–O(2)	120
As(2)–Ru–Cl(a)	90.3(2)	O(1)–N–Ru	123(2)
N–Ru–As(1)	86.0(11)	O(2)–N–Ru	117.2(14)
N–Ru–As(2)	85.4(11)		

Table 3 Selected bond distances (Å) and angles (°) for $trans\text{-}[\text{RuCl}(\text{pdma})_2(\text{NO})][\text{PF}_6]_2$

Ru–As(1)	2.4798(9)	Ru–N(1)	1.7500(2)
Ru–As(2)	2.4782(10)	N(1)–O(1)	1.243(14)
Ru–Cl(1)	2.199(4)		
As(1)–Ru–As(1a)	180.0	As(2)–Ru–As(2a)	180.0
As(1)–Ru–As(2)	84.85(3)	As(2)–Ru–Cl(1)	91.21(11)
As(1)–Ru–As(2a)	95.15(3)	As(2)–Ru–N(1)	88.84(3)
As(1)–Ru–Cl(1)	89.56(11)	As(2a)–Ru–Cl(1)	88.79(11)
As(1)–Ru–N(1)	90.41(2)	As(2a)–Ru(1)–N(1)	91.16(3)
As(1a)–Ru–Cl(1)	90.44(11)	Cl(1)–Ru–N(1)	179.91(8)
As(1a)–Ru–N(1)	89.60(2)	Ru–N(1)–O(1)	171.3(7)

Table 4 Selected bond distances (Å) and angles (°) for salt 2-dmf

Ru–As(1)	2.419(2)	Ru–As(4)	2.420(1)
Ru–As(2)	2.432(1)	Ru–Cl	2.436(3)
Ru–As(3)	2.431(2)	Ru–N	2.118(8)
As(1)–Ru–As(2)	84.28(5)	As(2)–Ru–N	92.8(2)
As(1)–Ru–As(3)	172.36(6)	As(3)–Ru–As(4)	84.71(5)
As(1)–Ru–As(4)	94.06(5)	As(3)–Ru–Cl	85.2(1)
As(1)–Ru–Cl	87.2(1)	As(3)–Ru–N	94.0(2)
As(1)–Ru–N	93.6(2)	As(4)–Ru–Cl	85.60(9)
As(2)–Ru–As(3)	96.07(5)	As(4)–Ru–N	93.8(2)
As(2)–Ru–As(4)	173.25(6)	Cl–Ru–N	179.0(2)
As(2)–Ru–Cl	87.78(9)		

Table 5 Selected bond distances (Å) and angles (°) for salt 11

Ru(1)–As(1)	2.4218(9)	Ru(2)–As(3)	2.4135(7)
Ru(1)–As(2)	2.4291(8)	Ru(2)–As(4)	2.4278(9)
Ru(1)–N(21)	2.121(4)	Ru(2)–N(41)	2.131(5)
As(1)–Ru(1)–As(1a)	180.0	As(3)–Ru(2)–As(3b)	180.0
As(1)–Ru(1)–As(2)	86.05(3)	As(3)–Ru(2)–As(4)	85.08(3)
As(1)–Ru(1)–As(2a)	93.95(3)	As(3)–Ru(2)–As(4b)	94.92(3)
As(1)–Ru(1)–N(21)	89.77(12)	As(3)–Ru(2)–N(41)	87.22(12)
As(1)–Ru(1)–N(21a)	90.23(12)	As(3)–Ru(2)–N(41b)	92.78(12)
As(2)–Ru(1)–As(2a)	180.0	As(4)–Ru(2)–As(4b)	180.0
As(2)–Ru(1)–N(21)	89.16(12)	As(4)–Ru(2)–N(41)	89.02(12)
As(2)–Ru(1)–N(21a)	90.84(12)	As(4)–Ru(2)–N(41b)	90.98(12)
N(21)–Ru(1)–N(21a)	180.0	N(41)–Ru(2)–N(41b)	180.0

quasi-reversible reduction waves are observed on cathodic scanning at -0.47 and -1.59 V *vs.* SCE. The two- and three-electron reduced forms of $trans\text{-}[\text{RuCl}(\text{pdma})_2(\text{NO})]^{2+}$ are evidently more stable than those of the related $trans\text{-}[\text{RuCl}(\text{bipy})_2(\text{NO})]^{2+}$ (bipy = 2,2'-bipyridine) and $trans\text{-}[\text{RuCl}(\text{py})_4(\text{NO})]^{2+}$, since the latter two complexes undergo rapid decomposition following two-electron reduction.^{19,20}

Salt 1–5, 7 and 9–11 all show reversible $\text{Ru}^{\text{III}}\text{-Ru}^{\text{II}}$ oxidation waves, the $E_{\frac{1}{2}}$ values of which vary predictably according to the nature of the axial ligands. The shift of +260 mV in the reduction potential on going from 7 to 9 reflects the marked stabilization of Ru^{II} relative to Ru^{III} caused by methylation of the pyrazine ligand. This is rather less than the analogous

Table 6 Crystallographic data and refinement details

	<i>trans</i> -[RuCl(NO ₂)(pdma) ₂]	<i>trans</i> -[RuCl(pdma) ₂ (NO)]-[PF ₆] ₂	2-dmf	11
Formula	C ₂₀ H ₃₂ As ₄ ClNO ₂ Ru	C ₂₀ H ₃₂ As ₄ ClF ₁₂ NOP ₂ Ru	C ₂₈ H ₄₄ As ₄ ClF ₆ N ₂ OPRu	C ₂₈ H ₄₄ As ₄ F ₁₂ N ₄ P ₂ Ru
<i>M</i>	754.67	1028.61	1005.84	1127.36
Crystal system	Monoclinic	Monoclinic	Monoclinic	Triclinic
Space group	<i>P</i> 2 ₁ / <i>n</i>	<i>P</i> 2 ₁ / <i>n</i>	<i>C</i> 2/ <i>c</i>	<i>P</i> $\bar{1}$
<i>a</i> /Å	8.862(2)	8.3250(6)	26.823(9)	11.943(3)
<i>b</i> /Å	9.316(2)	10.2621(19)	9.314(2)	12.389(3)
<i>c</i> /Å	15.773(3)	18.937(5)	31.083(5)	14.2307(17)
α /°				88.328(17)
β /°	99.77(2)	93.791(11)	101.17(2)	87.042(17)
γ /°				66.922(19)
<i>U</i> /Å ³	1283.3(5)	1614.3(5)	7618(3)	1934.5(7)
<i>Z</i>	2	2	8	2
<i>D_c</i> /Mg m ⁻³	1.953	2.116	1.754	1.935
<i>T</i> /K	120	153	303	153
λ /Å	1.541 78 (Cu-K α)	0.710 73 (Mo-K α)	1.541 78 (Cu-K α)	0.710 73 (Mo-K α)
<i>F</i> (000)	736	994.49	3968	1106.27
μ /mm ⁻¹	11.766	4.81	8.865	3.95
Scan type	θ -2 θ	ω	ω -2 θ	ω
2 θ limit/°	56.0	50.0	120.1	46.0
<i>h, k, l</i> Ranges	-9 to 9, 0-10, -1 to 16	-9 to 9, 0-12, 0-22	-24 to 30, -9 to 10, -34 to 34	-12 to 13, 0-13, -15 to 15
Reflections collected	2476	5109	6220	5984
Unique reflections (<i>R_{int}</i>)	1674 (0.036)	2829 (0.033)	6064 (0.029)	5409 (0.021)
Observed reflections	1403 [<i>I</i> > 2 σ (<i>I</i>)]	2458 [<i>I</i> > 2.5 σ (<i>I</i>)]	4012 [<i>I</i> > 3 σ (<i>I</i>)]	4414 [<i>I</i> > 2.5 σ (<i>I</i>)]
Final <i>R</i> indices ^a	<i>R</i> 1 = 0.0643, <i>wR</i> 2 = 0.2092	<i>R</i> = 0.054, <i>R'</i> = 0.080	<i>R</i> = 0.058, <i>R'</i> = 0.076	<i>R</i> = 0.033, <i>R'</i> = 0.044
(all data) ^a	<i>R</i> 1 = 0.0761, <i>wR</i> 2 = 0.2284	<i>R</i> = 0.067, <i>R'</i> = 0.083	<i>R</i> = 0.093, <i>R'</i> = 0.083	<i>R</i> = 0.048, <i>R'</i> = 0.047
Goodness of fit, <i>S</i>	1.128	2.65	2.02	1.52
No. parameters	145	188	352	464
Peak and hole/e Å ⁻³	1.714, -1.358	1.090, -0.950	1.02, -0.79	1.180, -0.530

^a For *trans*-[RuCl(NO₂)(pdma)₂]: *R*1 = $\Sigma(|F_o| - |F_c|)/\Sigma|F_o|$; *wR*2 = $[\Sigma w(F_o^2 - F_c^2)^2/\Sigma w(F_o^2)^2]^{1/2}$; *S* = $[\Sigma w(F_o^2 - F_c^2)^2/(M - N)]^{1/2}$ where *M* = number of reflections, *N* = number of parameters. For *trans*-[RuCl(pdma)₂(NO)][PF₆]₂, **2-dmf** and **11**: *R* = $\Sigma(|F_o| - |F_c|)/\Sigma|F_o|$; *R'* = $[\Sigma w(F_o - F_c)^2/\Sigma w F_o^2]^{1/2}$; *S* = $[\Sigma w(F_o - F_c)^2/(M - N)]^{1/2}$.

shift of +380 mV between [Ru(NH₃)₅(pyz)]²⁺ and [Ru(NH₃)₅(mpyz)]³⁺ in aqueous solution.¹⁶

The irreversible pyrazine reduction wave for salt **7** is shifted by +1.13 V, and becomes reversible, upon methylation to give **9**. This is due to the lowering of the π^* ligand LUMO energy, also reflected in the m.l.c.t. absorption maxima, coupled with the greater stability of the mpyz⁻ neutral radical compared with the pyz⁻ radical anion. The complex in **9** shows a second, irreversible reduction wave at -1.45 V *vs.* SCE. The dmsO complex in **6** shows an irreversible oxidation process on anodic scanning, followed by an irreversible reduction wave shifted by *ca.* -1 V. This behaviour is attributed to a redox-induced linkage isomerization of the dmsO ligand from S- to O-bound modes upon oxidation of Ru^{II} to Ru^{III}.²¹ The PPh₃ complex in **8** exhibits an irreversible Ru^{III}-Ru^{II} oxidation process, suggesting facile dissociation of the bulky phosphine ligand following oxidation to Ru^{III}.

Structural studies

Single-crystal structures were determined for the complex *trans*-[RuCl(NO₂)(pdma)₂] and for the salts *trans*-[RuCl(pdma)₂(NO)][PF₆]₂, *trans*-[RuCl(pdma)₂(py)][PF₆]₂·dmf (**2-dmf**) and *trans*-[Ru(pdma)₂(mim)][PF₆]₂ **11**. Representations of the complexes are shown in Figs. 1, 2, 3 and 4, respectively. These are the first reported structures for ruthenium complexes of the pdma ligand, although the structures of *cis*-[RuCl₂(CO)₂{1,2-(PhMeAs)₂C₆H₄}] and *trans*-[RuBr₂{1,2-(Me₂As)₂C₆F₄}₂]BF₄, featuring closely related arsine ligands, have been published.^{22,23}

All of the complexes show the expected *trans* arrangement of the pdma ligands, with an average Ru-As bond distance of 2.435 Å and an average As-Ru-As chelate angle of 85.03°. Comparison of the markedly different Ru-Cl bond distances of

2.448(9) Å in *trans*-[RuCl(NO₂)(pdma)₂] and 2.199(4) Å in *trans*-[RuCl(pdma)₂(NO)][PF₆]₂ amply demonstrates the established *trans*-shortening influence of the linearly bonded nitrosyl group.²⁴ The Ru-Cl bond distance in **2-dmf** is relatively long at 2.436(3) Å. The nitrosyl ligand in *trans*-[RuCl(pdma)₂(NO)][PF₆]₂ shows some distortion from purely linear bonding with a Ru-N(1)-O(1) angle of 171.3(7)°.

In salt **2-dmf** the plane of the pyridine ring is aligned with the long molecular axis, bisecting the As-Ru-As angles of the chelate units, presumably in order to minimize steric interactions with the methyl groups. A slight distortion of the pdma ligands away from the pyridine ring is evident with an average As-Ru-N angle of 93.6(2)°. The 1-methylimidazole rings in **11** are coplanar and orientated such that their planes bisect the As-Ru-As chelate angles. A symmetric distortion is evident with the pdma benzene rings tilting away from the 1-methylimidazole methyl groups.

Conclusion

The precursor *trans*-[RuCl(pdma)₂(NO)][PF₆]₂ readily affords derivatives *via* sequential substitution of the nitrosyl and chloride ligands in clean, high-yield reactions. No *trans-cis* isomerization or loss of the pdma ligands is observed. This chemistry is currently being used for the synthesis of functionalized mono- and bi-nuclear complexes based upon the *trans*-{Ru(pdma)₂}²⁺ centre, and will be applied to other related ruthenium complexes containing *trans*-Cl/NO ligands.

Acknowledgements

Thanks are due to the Nuffield Foundation for financial support and to Johnson Matthey plc for a generous loan of ruthenium trichloride.

References

- 1 A. Juris, V. Balzani, F. Barigelletti, S. Campagna, P. Belser and A. von Zelewsky, *Coord. Chem. Rev.*, 1988, **84**, 85; T. J. Meyer, *Acc. Chem. Res.*, 1989, **22**, 163; V. Balzani and F. Scandola, *Supramolecular Photochemistry*, Ellis Horwood, Chichester, 1991.
- 2 C. Creutz, *Prog. Inorg. Chem.*, 1983, **30**, 1; R. J. Crutchley, *Adv. Inorg. Chem.*, 1994, **41**, 273.
- 3 M. Schröder and T. A. Stephenson, in *Comprehensive Coordination Chemistry*, eds. G. Wilkinson, R. D. Gillard and J. A. McCleverty, Pergamon, Oxford, 1987, vol. 4.
- 4 P. G. Douglas, R. D. Feltham and H. G. Metzger, *J. Am. Chem. Soc.*, 1971, **93**, 84.
- 5 (a) S. A. Adeyemi, F. J. Miller and T. J. Meyer, *Inorg. Chem.*, 1972, **11**, 994; (b) S. A. Adeyemi, E. C. Johnson, F. J. Miller and T. J. Meyer, *Inorg. Chem.*, 1973, **12**, 2371; (c) B. J. Coe, T. J. Meyer and P. S. White, *Inorg. Chem.*, 1995, **34**, 593; (d) B. J. Coe, T. J. Meyer and P. S. White, *Inorg. Chem.*, 1995, **34**, 3600.
- 6 P. G. Douglas and R. D. Feltham, *J. Am. Chem. Soc.*, 1972, **94**, 5254.
- 7 J. G. Muller and K. J. Takeuchi, *Inorg. Chem.*, 1990, **29**, 2185.
- 8 M. S. Quinby and R. D. Feltham, *Inorg. Chem.*, 1972, **11**, 2468.
- 9 G. M. Sheldrick, SHELXS 86, *Acta Crystallogr., Sect. A*, 1990, **46**, 467.
- 10 G. M. Sheldrick, SHELXL 93, Program for Crystal Structure Refinement, University of Göttingen, 1993.
- 11 S. R. Parkin, B. Moezzi and H. Hope, *J. Appl. Crystallogr.*, 1995, **28**, 53.
- 12 TEXSAN-TEXRAY Structure Analysis Package, Molecular Structure Corporation, Houston, TX, 1985.
- 13 N. P. C. Walker and D. Stuart, *Acta Crystallogr., Sect. A*, 1983, **39**, 158.
- 14 E. J. Gabe, Y. Le Page, J.-P. Charland, F. L. Lee and P. S. White, *J. Appl. Crystallogr.*, 1989, **22**, 384.
- 15 C. K. Johnson, ORTEP: A Fortran thermal ellipsoid plot program, Technical report ORNL-5138, Oak Ridge National Laboratory, Oak Ridge, TN, 1976.
- 16 C. Creutz and H. Taube, *J. Am. Chem. Soc.*, 1973, **95**, 1086.
- 17 A. F. Schreiner, S. W. Lin, P. J. Hauser, E. A. Hopcus, D. J. Hamm and J. D. Gunter, *Inorg. Chem.*, 1972, **11**, 880.
- 18 R. W. Callahan and T. J. Meyer, *Inorg. Chem.*, 1977, **16**, 574.
- 19 H. Nagao, H. Nishimura, H. Funato, Y. Ichikawa, F. S. Howell, M. Mukaida and H. Kakihana, *Inorg. Chem.*, 1989, **28**, 3955.
- 20 H. Nishimura, H. Matsuzawa, T. Togano, M. Mukaida, H. Kakihana and F. Bottomley, *J. Chem. Soc., Dalton Trans.*, 1990, 137.
- 21 A. Yeh, N. Scott and H. Taube, *Inorg. Chem.*, 1982, **21**, 2542.
- 22 S. R. Hall, B. W. Skelton and A. H. White, *Aust. J. Chem.*, 1983, **36**, 271.
- 23 N. R. Champness, W. Levason, D. Pletcher and M. Webster, *J. Chem. Soc., Dalton Trans.*, 1992, 3243.
- 24 J. T. Veal and D. J. Hodgson, *Inorg. Chem.*, 1972, **11**, 1420; F. Bottomley, *J. Chem. Soc., Dalton Trans.*, 1974, 1600; 1975, 2538.

Received 5th June 1996; Paper 6/03925A